Diyala Journal of Engineering Sciences

ISSN 1999-8716

Printed in Iraq

Vol. 04, No. 02 , pp. 86-104, December 2011

CATALYTIC REFORMING OF HEAVY NAPHTHA, ANALYSIS AND SIMULATION

Dr. Zaidoon M. Shakoor

Lecturer/Chemical Engineering Department/University of Technology/ Baghdad

E-mail: dr_zaidoon@yahoo.com

(Received: 17/6/2010 ; Accepted:26/4/2011)

ABSTRACT:- In this paper, one-dimensional steady-state mathematical model of a semi regenerative naphtha catalytic reforming process had been made. This model incorporated a detailed kinetic model involving 24 components, 1 to 11 carbon atoms for paraffins (n and iso) and 6 to 11 carbon atom for naphthenes and aromatics with 71 reactions. The effect of pressure drop was considered through Ergun equation. The model explains the composition, temperature and pressure distributions along the four reforming reactors.

The simulation results of the proposed model were compared with the experimental results obtained from literature to validate the model.

The results showed good agreement between the reformate composition of proposed model with the experimental reformate composition.

Finally, the mathematical model was used to study the effect of reactor feed temperature, total pressure and hydrogen to hydrocarbon feed ratio on the reformate compositions.

Keywords: Heavy Naphtha, Reforming, Model, Simulation, MATLAB.

1. INTRODUCTION

Catalytic naphtha reforming is a very important process for producing high octane gasoline, aromatic feedstock and hydrogen in petroleum refining and petrochemical industries [(1)]. Catalytic reforming unit uses naphtha or cracking oil as feedstock to produce high octane value liquid as main products with hydrogen (H_2) and liquefied petroleum gas (LPG) as by-products [(2)].

A conventional naphtha reforming process consists of 3 or 4 reactors in series and heater before each reactor to reheat the stream into the reaction temperature range, before entering the next reactor. The reactors operate adiabatically at temperatures of 450-550°C, total pressures of 10-35atm, and molar hydrogen-to-hydrocarbon ratios (H_2/HC) of 3-8.

Catalytic reforming unit's uses industrial catalysts consisted of Gama Alumina support as acid function treated with chlorine in order to increase its surface acidity. The metal function is usually provided by platinum, of very small particles dispersed on the surface of catalyst, and its properties are fine-tuned by the addition of another element such as rhenium, ten, germanium, and iridium[(3)].

The major chemical reactions during the catalytic reforming are the following [(4)]:

1. Dehydrocyclization of paraffins into aromatics.
2. Isomerization of alkylcyclopentanes into cyclohexanes.
3. Dehydrogenation of cyclohexanes into aromatics.
4. Isomerization of linear paraffins into iso-paraffins.
5. Hydrocracking of naphthenes and paraffins.

6. Hydrodealkylation of aromatics;
7. Coke formation.

Some of these reactions are desired because of increasing octane number of gasoline. Cyclization and aromatization for paraffins are desired reactions because they increasing the number of branches and hence increase of octane number. The dehydrocyclization and dehydrogenation reactions produce hydrogen as by-product. On the other hand, hydrocracking and hydrodealkylation are mostly undesired reactions because they lower reformate and hydrogen yields also coke formation is undesired because its effect on catalyst deactivation [5].

2. KINETIC MODEL STUDIES

It is very important to choose an appropriate kinetic model capable of predicting the detailed reformate composition in order to use it, in combination with a catalytic reforming reactor model for simulation and optimization purpose.

First successful kinetic model for catalytic reforming process is proposed by Smith [6]. Smith model divided the naphtha feed into naphthenic, paraffinic and aromatic lumps with average carbon number properties. He also introduced hydrogen, ethane, propane, and butane into the system in addition to these groups.

Krane[7] developed his model, he assumed that the feed was consisted of 20 pseudo components and hydrocarbons from 6 to 10 carbon atoms. Moreover, reaction network was contained of 53 reactions.

Kmak[8] used Langmuir kinetic model for the first time for catalytic reforming process.

Taskar and Riggs [9] developed a more detailed model of a semiregenerative catalytic naphtha reformer, involving 35 pseudo components.

Unmesh and James [10] developed a kinetic model included 35 pseudo components in the reaction network, and 36 reactions.

In series of studies, Ancheyta et al.[11, 12,13] extended the work of Krane [7] by using a higher number of reactions, taking into account the benzene precursors of the feed, and the effect of pressure and temperature on the rate coefficients. In Ancheyta model, naphtha contained 1:11 paraffinic, 6:11 naphthenic and aromatic hydrocarbons. Indeed, the reaction of cyclohexane formation from cyclopentane and paraffins isomerization is considered in this model

Hu et al,[14, 15] studied of molecular modeling of catalytic reforming. They used molecular type homologous series matrices (MTHS) to represent the naphtha feed compositions. The reaction network involves 21 classes of molecules and 51 reactions. On the basis of the simulation model, they performed a process optimization for feed temperature and pressure under constraints such as benzene content, aromatic content and RON (research octane number) limitations.

Liang et al.,[2] proved their model assumptions, in which the temperature distribution is assumed only in axial direction in the reactors and all reactions within reforming process are assumed in homogeneous phase.

3. MATHEMATICAL MODEL

Mathematical modeling of the reactor is necessary to attain a proper process design and adequate prediction of the material and energy balance under different operating condition.

In the present mathematical model the following assumptions was considered:

1. The system is at state conditions.

2. The variation in the radial direction is negligible. Therefore, the compositions, temperature and pressure are only functions of axial direction [2].

3. All reactions are homogenous phase [2].

4. All reactions are pseudo first order with respect to hydrocarbon [11, 12, 13].

5. Plug flow in reactor.

The mathematical model equation results from application of material and energy balance principles in a differential volume. This leads to a set of ordinary, first-order differential equations that must be solved using numerical techniques to obtain concentration and temperature profile along the reactor as follow [16]:

$$-\frac{dC_i}{dZ} = \sum_{i=1}^{m} \frac{Mwt}{Z \times WHSV}(r_i) \qquad (1)$$

$$\frac{dT}{dZ} = \frac{S\sum_{i=1}^{m}(r_i)(-\Delta H_{Ri})}{\sum_{i=1}^{m} F_i Cp_i} \qquad (2)$$

Where: m represent the number of component in the mixtures.

All of researchers (Ancheyta et al.[11, 12, 13], Enrique et al. [16]) used the above two equations (1 and 2) to represent reformate composition and reactors temperature drop within the reforming process, but they don't take into consideration the pressure drop within the reforming process. In this research for the first time the Ergun [17] equation (3) was used for computing total differential pressure drop in axial flow reactor:

$$-\frac{dP_t}{dZ} = 1.7\times10^{-5}\frac{1-e}{e^3 \rho d_p}G^2 + 1.5\times10^{-3}\frac{(1-e)^2 m}{e^3 \rho d_p^2}G \qquad (3)$$

In order to evaluate the heat capacity the following correlation has been used;

$$Cp_i = A_i + B_i T + C_i T^2 + D_i T^3 \qquad (4)$$

The coefficients of heat capacity polynomial were taken from Reid et al. [18].

For each individual reactor within the process, numerical integration method was used to integrate the component mass balance, energy balance and pressure drop differential equations (1, 2 and 3) involved in this model. MATLAB 7 with the aid of fourth order Runge-Kutta integration command named ode15s was used to integrate 24 stiff ordinary differential equations for mass balance, while ode45 command was used to integrate the other two equations for heat and pressure drop equations. The flow chart for simulation program of naphtha reforming process is shown in Figure (1).

3.1. Simulation Condition

The derived model was tested compared to a commercial catalytic reforming unit composed of four reactors in series with inter-stage heater. The operating condition of this unit taken for simulation were as follows: 490 °C inlet temperature, 10 bar reactor pressure, hydrogen to oil ratio of 6.3 mol/mol, and feedstock flow rate of 30 MBPD [13].

The properties of the feedstock (hydrodesulfurized heavy naphtha) are given in Table (1) and the feed composition is presented in Table (2).

The length, diameter, catalyst-bed weight, and the corresponding weight hourly space velocities for each reactor are given in Table (3). As can be seen in this table the first reactor is always shorter than the other reactors and the last reactor is always the longest. This difference in the reactor sizes is because some of the reactions that occur in the first reactors are very fast, and those that take place in the last stages of reactors are slow [12].

3.2. Kinetic Model

All reactions within the process are assumed to be pseudo first order with respect to hydrocarbon and the kinetics were expressed by seventy-one first order reaction steps. The seventy-one kinetic parameter of the proposed kinetic model were estimated by Ancheyta et al [11]. All reaction steps are combined into twenty-four rate reaction equations (r_i), one for each component. Each reaction rate equation is a function of the kinetic constant (k_i) and the component concentration (C_i).

The naphtha feed to reforming process contain paraffin's, naphthenes, and aromatics with carbon number from 1 to 11 carbon atoms for paraffin's (P_1-P_{11}) and from 6 to 11 carbon atoms for naphthenes (N_6-N_{11}) and aromatics (A_6-A_{11}). The extended kinetic model employs a lumped mathematical representation of the seventy-one chemical reactions for all 24 lumps that taken place can be shown in Table (4) [12].

Other reactions taken into account in this kinetic model are cyclohexane formation via methycyclopentane isomerization (MCP↔N_6), MCP production from P6 (P_6↔MCP), and paraffin isomerization (n-P_i↔ iso-P_i) [12].

The effect of temperature and pressure on the kinetic constants can be expressed in equation (5) [19].

$$k_i = k_i^{\circ}\left[\frac{E_{Aj}}{R}\left(\frac{1}{T_{\circ}}-\frac{1}{T}\right)\right]\left(\frac{p_t}{p_{\circ}}\right)^{ak} \qquad (5)$$

The values of activation energy and pressure effect factors are given in Table (5).

4. MODEL VALIDATION

The composition profile of each component versus catalyst weight was shown in Figures (2, 3, 4 and 5). Predicted reformate composition profiles of total (n- and iso-) paraffins, naphthenes and aromatics are presented in Figure (2). Catalysts weight (kg) was chosen as a convenient parameter for indicating the reactor position as has been done by earlier workers [11, 12, 16]. Equation (6) was used to change the way of result displaying from reactor length to catalyst weight.

$$dw = S\rho_{cat}(1-e)dZ \qquad (6)$$

n-Paraffins, and iso-Paraffins compositions as a function of catalyst weight distribution is shown in Figures (3 and 4) respectively as well as naphthenes, and aromatics reformate compositions are presented in Figures (5) and (6) respectively.

From Figures (3) and (4) it can be seen, that the percentage of light paraffins (n-, and iso-P_5, and P_6) increased, because they are produced by hydrocracking or hydogenolysis. Also the same figure show that n-P_7 and iso-P_7 slightly decreases but heavier paraffins P_8-P_{11} (n-, and iso-) exhibited high levels of conversion especially in the 3rd and 4th reactor.

Figure (5) shows that naphthenes (N_6-N_{11}) react essentially to completion. The concentrations of (N_6-N_{11}) decreases as they undergo conversion. A high rate of conversion of naphthenes was found in the first and$_{89}$second reactors (N_6 and N_7) are almost totally converted. After third reactor, naphthenes compositions approach very low values.

The dehydrogenation of naphthenes and production of aromatics and hydrogen was the fastest among reforming reactions, therefore it nearly took place in 1st reactor and the variation of aromatics and naphthenes concentration were very significant. The increase in concentration of aromatics in the 2nd and 3rd reactors was basically due to the disappearance of paraffins. Hydrocracking of naphthenes and paraffins were slow and exothermic reactions, so these reactions take place often in 3rd reactor.

On the other hand, from Figure (6) it can be observed that as the feedstock pass through the unit the content of aromatic hydrocarbons are increased, also the increasing of light aromatics contents (A_6, A_7, A_8, and A_9), are faster than in heavier aromatics (A_{10}, and A_{11}).

Table (7) shows the difference between the reformate composition obtained by simulation and obtained in commercial reforming unit by Ancheyta et al.[12]. The maximum absolute difference between these two values is (2.28 mol %). It can be observed from this table that there are very good agreement between the simulated and reported values.

5. SIMULATION RESULTS

5.1 Reactor Temperature

Figure (7) shows the predicted temperature distribution along the reforming process. The major reforming reactions are highly endothermic producing a decrease in the temperature of the reaction stream and catalyst along the reactor. For this reason, commercial catalytic reformers are designed with multiple reactors and with heaters between the reactors to maintain reaction temperature at operable levels. As the feedstock passes through the sequence of heating and reacting, the reactions become less endothermic and temperature difference across the reactors decrease [20, 21].

In the first reactor, the major reactions are endothermic and very fast, such as dehydrogenation of paraffins and naphthenes to aromatics as can be seen in Figure (7), while in second reactor isomerization take place, the remaining naphthenes are dehydroisomerized and temperature drop is observed. The temperature drop through the third and fourth reactors were low compared to first two reactors, which is due to the exothermic of hydrocracking and dehydrocyclization reaction of paraffins. Table (8) shows the comparison between the actual and simulated temperature drop within the four reactors. It can be observed from this table, the present model prediction match very well with the information reported in the commercial reforming unit [12]. The maximum absolute difference between predicted and actual reactor temperatures is (6.51 °C) in second reactor while the minimum absolute difference between predicted and actual reactor temperatures is (2.41 °C) in first reactor.

5.2 Hydrogen Molar Flow rate

Figure (8) shows that, the hydrogen molar flow rates increase in four reactors in spite of difference in types of reactions through the unit. For given a naphtha feedstock the yield of hydrogen is determined by the balance between hydrogen producing and hydrogen-consuming reactions. Dehydrogenation and dehydrocyclization are the most important hydrogen- producing reaction [22, 23].

5.3 Reactor Pressure

Figure (9) shows the pressure drop along the four reactors. It can be observed from this figure, that the total pressure drop within the four reactors is mall (about 6 %) comparing to total reforming pressure, also there is a proportional relation between the drop in pressure and the reactor length or accumulated catalyst weight.

6. SELECTION THE BEST OPERATING CONDITIONS

Table (9) shows the effect of temperature, pressure, and hydrogen to naphtha molar ratio on reformate yield. The feed temperature for each reactor varied in the range of (460-540 °C). It can be observed that, increasing the feed temperature will increase aromatic yield which reaches maximum values at 540 °C.

According to the results presented in Table (10) it was observed that increasing the pressure does not change the reformate composition seriously. Increasing the pressure has a small effect on decreasing of aromatics and hydrogen content in reformate, because the dehydrogenation of naphthenes and dehydrocyclization of paraffins and reducing hydrocracking favored lower. The adverse effects of reduced pressure are increased catalyst coking and shorter cycle life, these conclusions is agreement with the work of Ali et al. [23].

Also, the H_2/HC ratio has little effect on the aromatics yield as shown in Table (11), while reducing H_2/HC ratio is useful in reducing energy costs for corresponding and circulating hydrogen and favors dehydrogenation of naphthene and dehydrocyclization of paraffins. Unfortunately reducing H_2/HC ratio can also increase catalyst coking and decrease catalyst activity and increase hydrocracking reaction.

7. CONCLUSIONS

The proposed mathematical model is suitable to study the effect of the reactors feed temperature, total pressure and hydrogen to hydrocarbon feed ratio on the reformate compositions. The calculated reformate composition agrees very well with experimental plant data.

Three process variables were studied as their effects on the reformate composition as follow.

- Increasing the reactors feed temperature will increase aromatic yield, which reach maximum values at 540 °C .
- Increasing the total pressure had a little effect on the decreasing the aromatics composition in the reformate.
- Increasing H_2/HC ratio had a little effect on the increasing aromatics composition in the reformate.

REFERENCES

1. Hu, Y.Y., Su, H.Y., Chu, J., (2002), "The research summarize of catalytic reforming unit simulation", Contr. Instrum. Chem. Ind., 29(2), 19-23.
2. Liang, K. M., Guo H. Y. Pan S. W., (2005), "A study on Naphtha Catalytic Reforming Reactor Simulation and Analysis", Journal of Zhejiang University Science, 6B(6), 590-596.
3. Seif, M.S.R., Zahedi, S., Sadighi, S., Bonyad, H., (2006), "Reactor Modeling and Simulation of Catalytic Reforming Process", J. Petroleum and Coal, vol 48, No3, 28-35.
4. Parera, J.M., Figoli, N.S., (1995), "Catalytic Naphtha Reforming" , Antos G.J., Aitani A.M., Parera J.M., Eds,. Marcel Dekker, New York, p. 45.
5. Hughes, T.R., Jacobson, R.L., Tamm, P.W., (1988), "Catalysis", (J.W. Ward, Ed.), Elsevier, Amsterdam, Netherlands, p. 317.
6. Smith, R.B., (1959), "Kinetic Analysis of Naphtha Reforming with Platinum Catalyst", Chem.Eng.Prog. , 55 (6), 76-80.
7. Krane, H.G., (1959), "Reactions in Catalytic Reforming Naphtha", Proceeding of the 5th World Petroleum Congress, 39- 51.
8. Kmak, W. S., Stuckey, A. N., (1973), "In Powerforming Process Studies with a Kinetic Simulation Model, AIChE National Meeting, Paper No.56a, New Orleans, March.
9. Taskar, U., Riggs, J.B., (1997), "Modeling and optimization of a semiregenerative catalytic naphtha reformer", AIChE J., 43, 740-753.

10. Unmesh, T., James, J. B., (1997), " Modelling & Optimization of Semi Regenerative Catalytic Naphtha Reformer " , AIChE J., 43 (3), 740-753.
11. Ancheyta, J., Villafuerte-Macias, E., (2000), "Kinetic Modeling of Naphtha Catalytic Reforming Reactions", Energy Fuels, 14, 1032-1037.
12. Ancheyta, J., Villafuerte, E., Diaz, L., Gonzalez, E., (2001), "Modeling and Simulation of Four Catalytic Reactors in Series for Naphtha Reforming. Energy Fuels, 15, 887-893.
13. Ancheyta, J., Villafuerte, E., Schachat, P., Aguilar, R., Gonzalez, E., (2002), "Simulation of a Commercial Semiregenerative Reforming Plant Using Feedstocks with and without Benzene Precursors", Chem. Eng. Technol., 25, 541-546.
14. Hu, S., Towler, G., Zhu, X. X. Combine, (2002), "Molecular Modeling with Optimization to Stretch Refinery Operation", Ind. End. Chem. Res., 41, 825.
15. Hu, S. Y., Zhu, X. X., (2004), "Molecular Modeling and Optimization for Catalytic Reforming" Chem. Eng. Commun., 191, 500-512.
16. Enrique, A.R., Ancheyta j.j., (1994), "New Model Accurately Predicts Reformer Composition", Oil and Gas J, Jan 31, 93-95.
17. Bird, R. B., Stewart, W. E., Lightfoot, E. N., (1960), "Transport Phenomena", Wiley: New York.
18. Reid, R. C., Prausnitz, J. M. and Poling, B. E., (1987), "The Properties of Gases and Liquids", McGraw-Hill Book Company,4 th edition.
19. Jenkins J.H., Stephens T.W., (1980), "Kinetics of Catalytic Reforming", J. Hyd. Proc, Nov, 163-167.
20. Hu Y.Y., Su. H.Y., Chu. J., (2003), "Modeling and Simulation of Commercial Catalytic Reformers", J. of Che. Eng. of Chines Univ, vol, 17, 418-424.
21. Weifeng H., Hongye, S., Hongyou, H., Jain C., (2006), "Modeling, Simulation and Optimization of a Whole Industrial Catalytic Naphtha Reforming Process on Aspen Plus Platform", Chin. J. Chem. Eng, vol 14, No 55, 584-591.
22. Weifeng H., Young H., Hongye S., Jain C., June (15-19), (2004), "Simulation, Sensitivity Analysis and Optimization of a Continuous Catalytic Reforming Process", Proceeding of the 5th World Congress on Intelligent Control and Automation.
23. Ali S.A., Siddiqui M.A., Mohammed A .A., (2006), "Parametric Study of Catalytic Reforming Process", J. React .Kinet. Catal. Litt, 87(1), 199-206.

NOMENCLATURE

A	Aromatics	(-)
C_i	Concentration of species i	mole/cm^3
C_P	Specific heat	J/mole.K
d_p	Equivalent diameter of a catalyst particle	m
e	Void fraction of reactor bed	m^3/m^3
E_A	Activation energy	kcal/mole
F.B.P	Final boiling point	(-)
F_i	Molar flow rate of species i	mole/hr
G	Total mass flux of fluid	kg.s/m^2
I.B.P	Initial boiling point	(-)
iso-P	Iso Paraffin	(-)
k°_i	Pre-exponential factor	(-)
k_i	Reaction rate constant	hr^{-1}
m	Viscosity	pa.s
Mwt	Molecular weight	g/gmole
MBPD	Million barrels per day	(-)
MCP	Methylcyclopentane	(-)
N	Naphthene	(-)
n-P	Normal Paraffin	(-)
P	Paraffin	(-)
P^o	Partial pressure	bar
P_t	Total pressure	bar
R	Gas constant	J/mole.K
r_i	Reaction rate of species i	mole/gcat. hr
S	Cross sectional area of reactor	m^2
T	Reaction temperature	°C
T^o	Initial temperature	°C
w	Catalyst weight	k
WHSV	Weight hour space velocity	hr^{-1}
Z	Length of reactor	m
ΔH_{Ri}	Heat of ith reaction	J/ mole
αk	Pressure effect	(-)
ρ	Reformate density	Kg/m^3
ρ_{cat}	Catalyst density	Kg/m^3

Table (1): Properties of the naphtha feedstock [12].

Property	
specificgravity 60/60	0.7406
molecular weight	104.8
IBP	88
10 vol %	101
90 vol %	155
FBP	180
total paraffins mol%	59.11
total naphthenes	20.01
total aromatics	20.88

Table (2): Naphtha feedstock molar composition [12]**.**

	n-Paraffins	**iso-Paraffins**	**Naphthenes**	**Aromatics**
C5	0.40	0.45	0.16 (MCP)	0.00
C6	3.60	7.30	4.00	1.10
C7	3.46	11.5	5.30	3.90
C8	3.20	10.8	4.00	7.05
C9	3.50	6.80	5.40	5.45
C10	5.40	0.00	1.15	2.48
C11	2.70	0.00	0.00	0.90
total	22.26	36.85	20.01	20.88

Table (3): Reactors specifications. [12]

Reactor	**Length (m)**	**Diameter (m)**	**Catalyst weight (ton)**	**WHSV (h^{-1})**
1	4.902	2.438	9.13	16
2	5.41	2.819	13.82	10.6
3	6.452	2.971	22.82	6.4
4	8.208	3.505	42.58	3.4

Table (4): Reactions of the kinetic model. [12]

Number of Reactions	
Paraffin's	
$P_n \rightarrow N_n$	6
$P_n \rightarrow P_{n-j} + P_j$	26
subtotal	32
Naphthenes	
$N_n \rightarrow A_n$	6
$N_n \rightarrow N_{n-j} + P_j$	11
$N_n \rightarrow P_n$	7
subtotal	24
Aromatics	7
$A_n \rightarrow A_{n-j} + P_j$	5
$A_n \rightarrow P_n$	1
$A_n \rightarrow N_n$	13
subtotal	
Total	71
n: Number of atoms of carbon ($1 \leq i \leq 5$)	

Table (5): Pressure effect and activation energy on reaction rate. [19]

Reactions	**a_k**	**Activation Energy**
isomerization	0.37	21
dehydrocyclization	-0.7	45
hydrocracking	0.433	55
hydrodealkylation	0.5	40
dehydrogenation	0.0	30

Table (6): Kinetic constants of the kinetic model. [11]

Reaction Step	**k**	**Reaction Step**	**k**	**Reaction Step**	**k**
$P_{11} \longrightarrow N_{11}$	0.0356	$P_8 \longrightarrow 2P_4$	0.0070	$N_8 \longrightarrow N_7+P_1$	0.0007
$P_{10} \longrightarrow N_{10}$	0.0243	$P_7 \longrightarrow P_6+P_1$	0.0027	$N_{11} \longrightarrow A_{11}$	0.6738
$P_9 \longrightarrow N_9$	0.0500	$P_7 \longrightarrow P_5+P_2$	0.0018	$N_{10} \longrightarrow A_{10}$	0.3198
$P_8 \longrightarrow N_8$	0.0266	$P_7 \longrightarrow P_4+P_3$	0.0043	$N_9 \longrightarrow A_9$	0.2205
$P_7 \longrightarrow N_7$	0.0076	$P_6 \longrightarrow P_5+P_1$	0.0018	$N_8 \longrightarrow A_8$	0.2150

$P_6 \longrightarrow N_6$	0.0000	$P_6 \longrightarrow P_4+P_2$	0.0016	$N_7 \longrightarrow A_7$	0.0788
$P_{11} \longrightarrow MCP$	0.0042	$P_6 \longrightarrow 2P_5$	0.0025	$N_6 \longrightarrow A_6$	0.1368
$P_{11} \longrightarrow P_{10}+P_1$	0.0075	$P_5 \longrightarrow P_4+P_1$	0.0018	$A_{11} \longrightarrow P_{11}$	0.0016
$P_{11} \longrightarrow P_9+P_2$	0.0100	$P_8 \longrightarrow P_3+P_2$	0.0022	$A_{10} \longrightarrow P_{10}$	0.0016
$P_{11} \longrightarrow P_8+P_3$	0.0135	$N_{11} \longrightarrow P_{11}$	0.0050	$A_9 \longrightarrow P_9$	0.0016
$P_{11} \longrightarrow P_7+P_4$	0.0135	$N_{10} \longrightarrow P_{10}$	0.0054	$A_8 \longrightarrow P_8$	0.0011
$P_{11} \longrightarrow P_6+P_5$	0.0191	$N_9 \longrightarrow P_9$	0.0054	$A_7 \longrightarrow P_7$	0.0016
$P_{10} \longrightarrow P_9+P_1$	0.0015	$N_8 \longrightarrow P_8$	0.0025	$A_{11} \longrightarrow A_{10}+P_1$	0.0006
$P_{10} \longrightarrow P_8+P_2$	0.0054	$N_7 \longrightarrow P_7$	0.0019	$A_{11} \longrightarrow A_9+P_2$	0.0006
$P_{10} \longrightarrow P_7+P_3$	0.0160	$N_6 \longrightarrow P_6$	0.0204	$A_{10} \longrightarrow A_9+P_1$	0.0006
$P_{10} \longrightarrow P_6+P_4$	0.0095	$MCP \longrightarrow P_6$	0.0008	$A_{10} \longrightarrow A_8+P_2$	0.0006
$P_{10} \longrightarrow 2P_5$	0.0095	$N_{11} \longrightarrow N_{10}+P_1$	0.0134	$A_{10} \longrightarrow A_7+P_3$	0.0000
$P_9 \longrightarrow P_8+P_1$	0.0030	$N_{11} \longrightarrow N_9+P_2$	0.0134	$A_9 \longrightarrow A_8+P_1$	0.0005
$P_9 \longrightarrow P_7+P_2$	0.0039	$N_{11} \longrightarrow N_8+P_3$	0.0080	$A_9 \longrightarrow A_7+P_2$	0.0005
$P_9 \longrightarrow P_6+P_3$	0.0068	$N_{10} \longrightarrow N_9+P_1$	0.0134	$A_8 \longrightarrow A_7+P_1$	0.0001
$P_9 \longrightarrow P_5+P_4$	0.0058	$N_{10} \longrightarrow N_8+P_2$	0.0134	$A_6 \longrightarrow N_6$	0.0015
$P_8 \longrightarrow P_7+P_1$	0.0019	$N_{10} \longrightarrow N_7+P_3$	0.0080	$MCP \longrightarrow N_6$	0.0238
$P_8 \longrightarrow P_6+P_2$	0.0056	$N_9 \longrightarrow N_8+P_1$	0.0127	$N_6 \longrightarrow MCP$	0.0040
$P_8 \longrightarrow P_5+P_3$	0.0034	$N_9 \longrightarrow N_7+P_2$	0.0127		

Table (7): Actual and simulated reformate compositions.

	Actual	**Simulated**	**Absolute difference**
n-P_5	2.6300	3.4802	0.8502
n-P_6	5.1300	3.8545	1.2755
n-P_7	2.8000	2.0358	0.7642
n-P_8	1.0400	0.5672	0.4728
n-P_9	0.5400	0.9153	0.3753
n-P_{10}	0.1500	2.0250	1.8750
n-P_{11}	0.0100	0.0489	0.0389
i-P_5	2.2000	3.8886	1.6886
i-P_6	9.9500	7.8889	2.0611
i-P_7	8.4000	7.7786	0.6214
i-P_8	3.7500	1.8493	1.9007
i-P_9	1.7600	0.0000	1.7600
i-P_{10}	0.0000	0.0000	0.0000
MCP	1.2500	1.6446	0.3946
N_6	0.1900	0.2513	0.0613
N_7	0.3800	1.1127	0.7327
N_8	0.5900	0.3416	0.2484
N_9	0.1400	0.1895	0.0495
N_{10}	0.0200	0.1347	0.1147
N_{11}	0.0000	0.0024	0.0024
A_6	5.4300	5.3470	0.0830
A_7	15.030	13.067	1.9623
A_8	18.630	19.564	0.9345
A_9	13.680	15.960	2.2800
A_{10}	4.7200	6.3710	1.6510
A_{11}	1.5800	1.6808	0.1008

Table (8): Actual and Predicted temperature drop along the reactors.

Reactor	**Actual ΔT °C**	**Simulated ΔT °C**	**Absolute difference °C**
1	53	50.5863	2.4137
2	30	36.5143	6.5143
3	17	22.3630	5.3630
	13	10.0815	2.9185

Table (9): Influence of reaction temperature on reformates composition.

Temperature °C	Pressure bar	H_2/HC ratio	n-Paraffins	iso-Paraffins	Naphthenes	Aromatics
460	10	6.3	16.03	30.76	4.30	48.91
480	10	6.3	13.49	25.63	3.82	57.06
495	10	6.3	12.93	21.41	3.68	61.99
500	10	6.3	13.21	20.49	3.68	62.61
520	10	6.3	12.12	16.14	3.05	68.69
540	10	6.3	9.480	6.150	1.74	82.63

Table (10): Influence of total pressure on reformate composition.

Temperature	Pressure bar	H_2/HC ratio	n-Paraffins	iso-Paraffins	Naphthenes	Aromatics
500	6	6.3	12.88	20.08	3.71	63.33
500	8	6.3	13.11	20.37	3.69	62.83
500	10	6.3	13.21	20.49	3.68	62.61
500	15	6.3	13.31	20.61	3.67	62.41
500	20	6.3	13.34	20.65	3.67	62.34
500	30	6.3	13.37	20.68	3.67	62.29
500	40	6.3	13.37	20.69	3.67	62.27

Table(11): Influence of hydrogen to hydrocarbon feed ratio on reformate composition.

Temperature °C	Pressure bar	H2/HC ratio	n-Paraffins	iso-Paraffins	Naphthenes	Aromatics
500	10	3	13.28	21.03	3.68	62.01
500	10	4	13.25	20.84	3.68	62.22
500	10	5	13.23	20.68	3.68	62.41
500	10	6	13.22	20.53	3.68	62.57
500	10	7	13.21	20.41	3.68	62.71
500	10	8	13.20	20.29	3.68	62.83

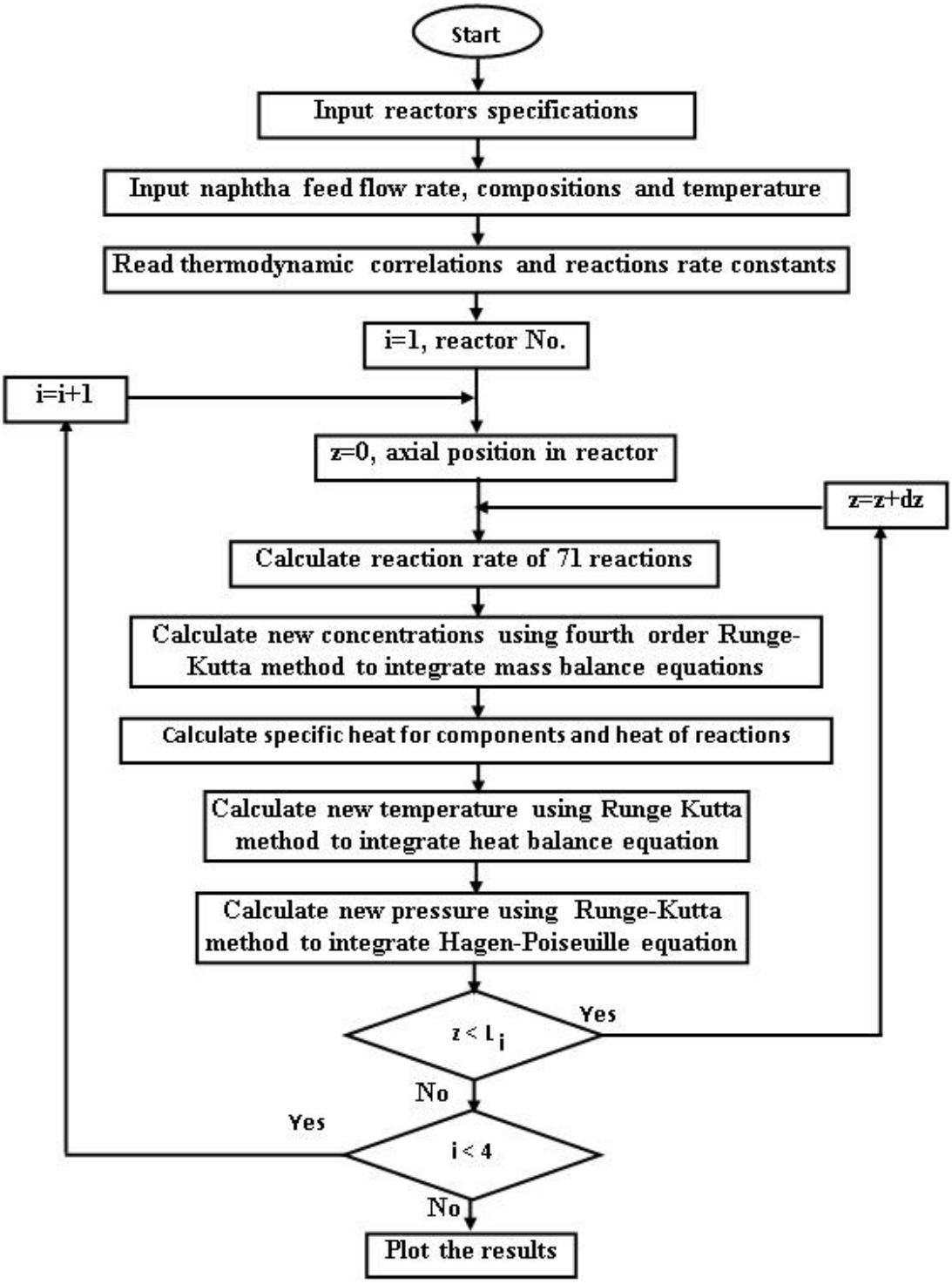

Fig.(1): Flow chart for fixed bed reactor simulation program

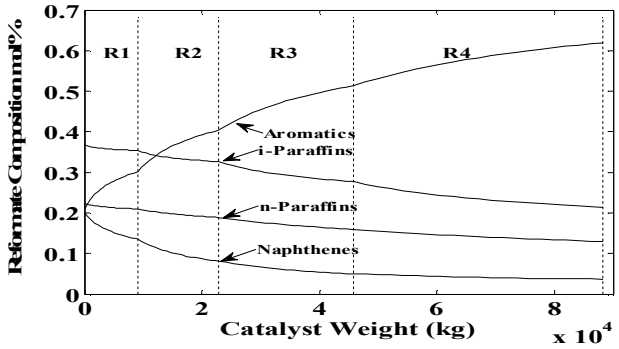

Fig.(2): Predicted composition profile of total n-Paraffins, iso-Paraffins, naphthenes, and aromatics in reforming process

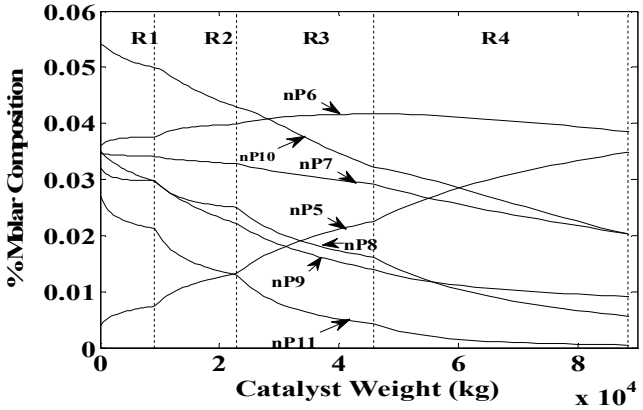

Fig.(3): Predicted n-Paraffins composition profile in reforming process.

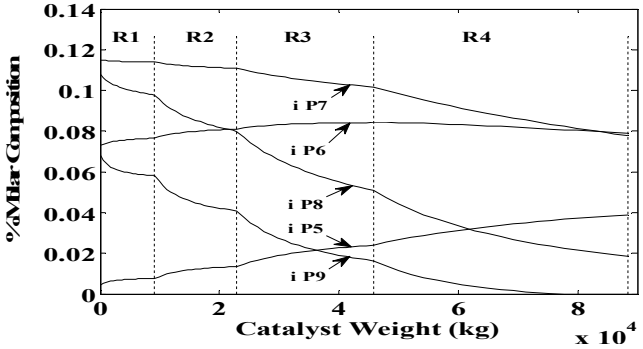

Fig.(4): Predicted naphthenes composition profile in reforming process

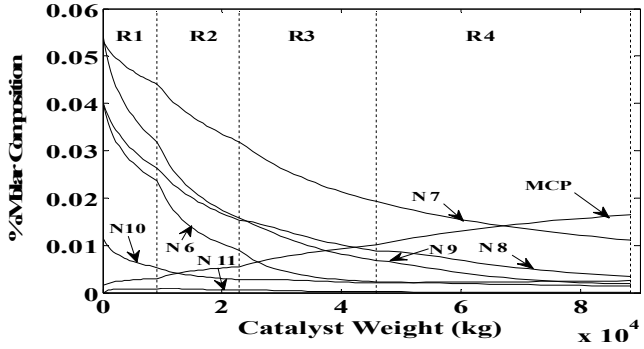

Fig. (5): Predicted iso-Paraffins composition profile in reforming process

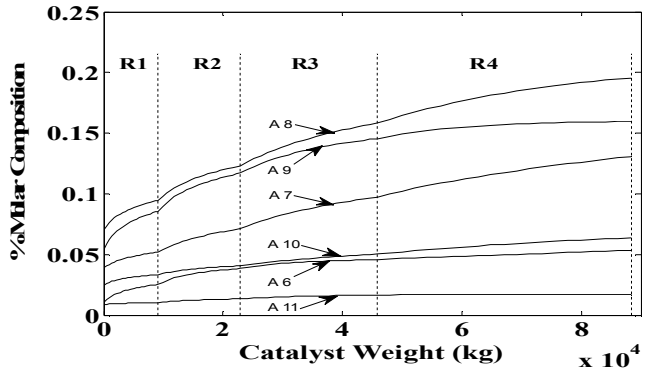

Fig.(6): Predicted aromatics composition profile in reforming process.

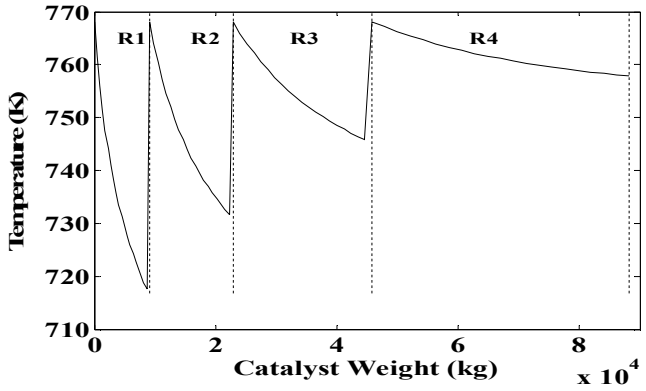

Fig.(7): Predicted temperature profile in reforming process.

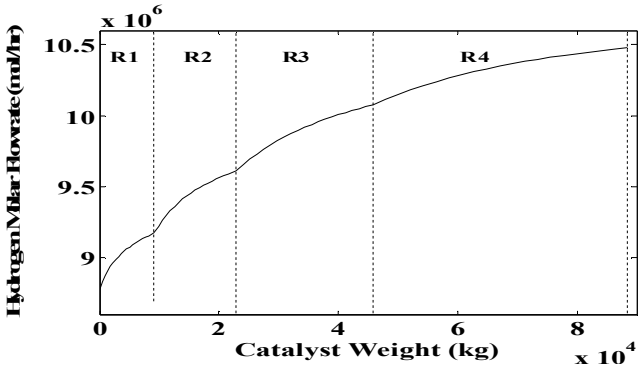

Fig.(8): Predicted hydrogen molar flow rate in reforming process

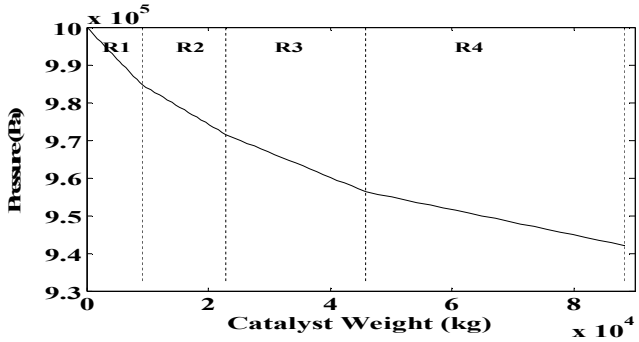

Fig.(9): Predicted pressure drop in reforming process.

تحليل ومحاكاة عملية التهذيب للنفثا الثقيلة

د.زيدون محسن شكور

الجامعة التكنولوجية / قسم الهندسة الكيمياوية

الخلاصة

تم في هذا البحث عمل موديل رياضي لمحاكاة عملية التهذيب مرحلية التنشيط للنفثا في الحالة المستقرة ولبعد واحد. الموديل الرياضي يتضمن وصف ٢٤ مادة وهي البرافينات (الايزو والنورمال) التي تحتوي من١ الى ١١ ذرة كاربون والنفثينات والمواد الاروماتية التي تحتوي من ٦-١١ ذرة كاربون بالاعتماد على ميكانيكية من ٧١ تفاعل. الموديل الرياضي يصف تغير التراكيز والضغط ودرجة الحرارة على طول المفاعلات الاربعة المستخدمة لعملية التهذيب.

لاختبار الموديل الرياضي تم مقارنة النتائج الرياضية المستحصلة من الموديل الرياضي مع نتائج عملية ماخوذة بنفس الظروف حيث كان هناك انطباق جيد بين نتائج الموديل الرياضي والنتائج العملية وكذلك هناك انطباق جيد بين تراكيز التهذيب النظرية والعملية. في النهاية تم دراسة تأثير الضروف التشغيلية وهي درجة الحرارة والضغط ونسبة الهيدروجين الى المواد الهيدروكاربونية على تراكيز التهذيب.